Turkish Journal of Electrical Engineering & Computer Sciences

http://journals.tubitak.gov.tr/elektrik/

Research Article

Turk J Elec Eng & Comp Sci
(2022) 30: 1715 – 1725

doi:10.55730/1300-0632.3900

On the performance analysis of flexible pairing between UAV and GU in NOMA

Man Hee LEE, Soo Young SHIN*
Department of IT Convergence Engineering, Kumoh National Institute of Technology
Gumi, South Korea

Received: 15.10.2021 • **Accepted/Published Online:** 27.02.2022 • **Final Version:** 22.07.2022

Abstract: The wireless communications regarding unmanned aerial vehicles (UAVs) have been investigated for the usage of base stations (BS) to provide Internet access. This paper presents the usage of a UAV as a pairing user to enhance the sum capacity by flexible pairing in nonorthogonal multiple access (NOMA). In the proposed scheme, the UAVs and the ground users (GUs) get paired to promote the line-of-sight (LoS) characteristics. The performance of flexible pairing is presented in terms of sum capacity, outage probability, and throughput with the LoS path loss. Channel modeling is necessary to apply flexible pairing by utilizing the LoS characteristic as a special case. Moreover, the height of the UAV is calculated based on the elevation angle. It is revealed that the LoS path loss determines the effect on the channel covariance. The analysis of the flexible pairing is shown with Monte Carlo-based simulation and analytic results are validated to maximize throughput.

Key words: Nonorthogonal multiple access (NOMA), unmanned aerial vehicle (UAV), ground user (GU), ergodic sum capacity, throughput

1. Introduction

In 6G networks, a combination of 5G services leads to extreme coverage and data rate superior to that of 5G [1]. One requirement of 6G network is the capacity which is satisfied with applying advanced wireless transmission technology [2]. In recent years, nonorthogonal multiple access (NOMA) has been recommended as the predominant and leading radio access technology (RAT) to increase system capacity and connection densities in 3rd Generation Partnership Project (3GPP) [3]. NOMA utilizes nonorthogonal resources to overcome a limited number of available channel resources. Its superiority has been demonstrated in terms of the overall system capacity and simple decoding structure, i.e. successive interference cancellation (SIC) [4]. In general, one pairing for two users are typical in NOMA for downlink scenario because of the decoding complexity and bit error rate (BER) performance [5–7]. Additionally, massive connectivity is required to support a large number of devices in the Internet of Things (IoT) networks. Unmanned aerial vehicle (UAV) has made an appearance to support massive connectivity.

Recently, UAV communication networks have attracted interest and been investigated in the literature [8, 9]. UAV communication network brings various benefits such as the flexibility of deployment, coverage, throughput and energy efficiency. The performance is improved by optimizing parameters such as bandwidth control, power allocation, UAV placement, and UAV trajectory.

*Correspondence: wdragon@kumoh.ac.kr

Among these perspectives, UAV placement is one of critical problems to solve and compromise network. The conventional communication is operated in a rich scattering environment with multiple communicating antennas and connected users. Otherwise, a UAV allows communication within a poor scattering environment. Moreover, the link reliability in the UAV network is affected by the location and height of the UAV. Due to battery issue on the UAV, the UAV generally relies on equipping the single antenna in [10, 11].

1.1. Related work

The related works have investigated on the handling UAVs with NOMA to satisfy the high data rate and broad coverage [12–15]. In [16], optimization problems for placement and power allocation (PA) were jointly proposed. In [17], a max-min rate optimization problem was proposed with constraints such as UAV altitude, transmit antenna bandwidth, PA, and bandwidth allocation for multiple users. In [18], a 3-D UAV framework, which was utilized with a stochastic geometry model, was proposed to provide wireless services.

The earlier research on UAV–NOMA networks has focused on the extension of transmit range and multiple connection over the cells. UAV is employed for BS and provides wireless services for other users over the cells [19, 20]. Otherwise, the role of UAV as a serving user also is needed as a direction of research. For this approach, a strategy of UAV placement and other pairing schemes are necessary to be prescribed and considered. Herein, a strategy for flexible pairing is proposed for a UAV and ground users (GUs) according to the UAV's location; height and distance from BS. Flexible pairing allows users to switch own roles based on capacity maximization and channel modeling.

1.2. Contributions

In this paper, the UAV is utilized as a user to get paired with static GUs. We assume that the routine of a UAV is limited within a cell for surveillance purposes. The GUs are assumed as IoT devices which is located to support UAV's surveillance. Flexible pairing is proposed for the UAV routine and the optimization problem is solved according to the UAV's location. Channel modeling is proposed to maximize the line-of-sight (LoS) characteristic.

Principal contributions of the paper are as follows:

- This paper investigates the issues that arise due to the different roles of the cell center user (CCU) and the cell edge user (CEU). It is assumed that GUs are IoT devices to equip single antenna and a UAV flies within a cell.
- Two scenarios are considered based on the location of a UAV and a GU. For these scenarios, we analyze the performances on the system model according to LoS effects on a CCU and a CEU.
- The performances are derived and validated in terms of sum capacity, outage probability, and throughput through simulation and analytical results.

1.3. Remainder of the paper

The remainder of this paper is organized as follows. Section 2 discusses the system model in which channel modeling and flexible pairing are shown using the outage probability and throughput, respectively. The results are presented in Section 3, including the outage probability and throughput-varying conditions. Section 4 presents the conclusions drawn from this research.

2. System model

The system model indicates that the routine of a UAV is limited within a cell for surveillance purposes. The GUs are assumed as IoT devices which has single antenna because of battery issue. The UAV moves in the same direction for simplification. However, it does not maneuver at the same velocity to make variations in the UAV's location. Following this assumption, a UAV can be a CCU or CEU depending on its distance from the BS. Figure. 1 illustrates the cell scenario involving a single UAV and multiple GUs, which communicates using the NOMA principle. It is assumed that the BS serves a single UAV and multiple GUs equipped with one receive antenna. The received signal for ith user is expressed as follows:

$$y_i = h_i \sum_{i=1}^{N} \sqrt{\rho \phi_i} x_i + n_i, \tag{1}$$

where h_i is the Rayleigh fading channel for ith user, x_i is the transmitted signal for ith user and n_i denotes the additive white Gaussian noise (AWGN) with zero mean and variance σ^2 for ith user. In addition, ρ is the transmitted power from BS and ϕ_i is PA coefficient for ith user.

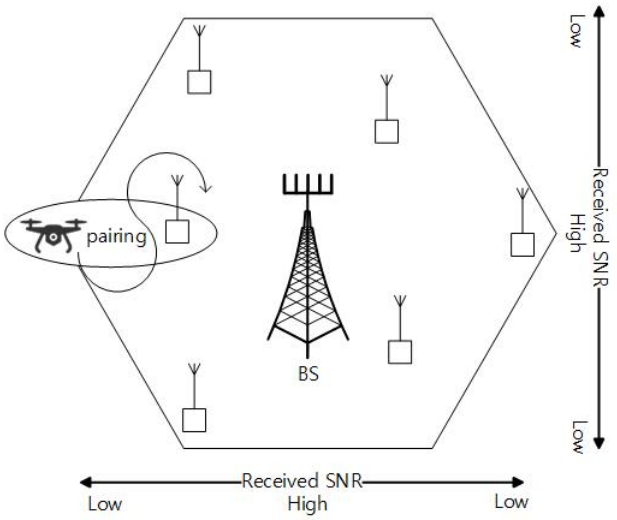

Figure 1. System model.

Following the NOMA principle, the users share same frequency resources that experience interference where a CCU and a CEU have a single pairing. To reduce the interference, SIC is performed at the CCU decoding CEU signal because a higher PA coefficient is assigned to the CEU. While the CEU receives less interference from the lower PA coefficient, the CEU deals with the CCU signal as noise. The K number of CEUs and $(N-K)$ number of CCUs are assumed in the proposed system. The received signal-to-interference-noise-ratio (SINR) for the ith CEU $(1 \leq i \leq N-K)$ is expressed as

$$\Gamma_i = \frac{\rho |h_i|^2 \phi_i}{\rho |h_i|^2 \sum_{j=i+1}^{K} \phi_j + \sigma^2}. \tag{2}$$

The received signal-to-noise ratio (SNR) for the ith CCU ($K \leq i \leq N$) is expressed as

$$\Gamma_i = \frac{\rho |h_i|^2 \phi_i}{\sigma^2}. \tag{3}$$

From eqs. (2) and (3), the capacity for the ith user can be expressed as

$$R_i = \log_2(1 + \Gamma_i). \tag{4}$$

2.1. Channel modeling

As shown in Figure 1, there are two types of channels in the networks: the U2G channel (from a UAV to a GU) and the G2U channel (from a GU to a UAV). Both channels have an LoS environment and surrounding buildings, similar to the standardized terrestrial communication. The elevation angle is used to calculate the height of the UAV based on the distance and is given by

$$\theta_i = \arctan\left(\frac{d_{v,i}}{d_{h,i}}\right), \tag{5}$$

where $d_{v,i}$ is the vertical distance which means height for ith user and $d_{h,i}$ is the horizontal distance for ith user, respectively.

The U2G and G2U channels can have LoS or non-LoS (NLoS) circumstances owing to the location of the UAV. Without considering the carrier frequency, the approximate path loss model is given by [21, 22]

$$P_L(d_{v,i}) = 10\alpha \log_{10}(d_{v,i}) + \beta(\theta_i), \tag{6}$$

where $\beta(\theta_i)$ is a constant for LoS path loss which is decided by elevation angle and α is the path loss exponent.

From the approximate path loss model, the channel variance is calculated using the path loss exponent and received signal strength. From eq. (6), the UAV is expected to be placed in better channel conditions than the GU because of the LoS path loss. The channel variance is used to calculate the ergodic capacity, which increases when the channel variance and distance of ith user are decreased. In this channel modeling, it is assumed that antenna characteristics do not affect the path loss.

2.2. Flexible pairing

Following the proposed system model, the UAV flexibly moves between the distributed GUs. At the specific point, the role between CCU and CEU is changed depending on the distance. Without loss of generality, the number of users for the pairing is typically limited to two. But the sum capacity can be improved by altering the height of the UAV and PA coefficients. In this regard, achievable capacity for the CCU and CEU from [23] can be expressed as follows:

$$\begin{aligned} R_1 &= \log_2(1 + \Gamma_1) = \log_2(1 + \rho\phi_1 |h_1|^2) \\ R_2 &= \log_2(1 + \min(\Gamma_2, \Gamma_{2\to 1})) \\ &= \log_2\left(1 + \min\left(\frac{\rho\phi_2 |h_2|^2}{\rho\phi_1 |h_2|^2 + 1}, \frac{\rho\phi_2 |h_1|^2}{\rho\phi_1 |h_1|^2 + 1}\right)\right). \end{aligned} \tag{7}$$

2.2.1. Outage probability

In this subsection, a closed form for the outage probability of the CCU and CEU is derived. The outage probability is defined as the cumulative distribution function (CDF) of the received SNR/SNIR evaluated at the rate threshold, γ_{th} because of the variable channel capacity. Additionally, the outage probability includes the connectivity parameter between the UAV and the GU because of avoiding the binary problem for connectivity. The CCU and CEU of exact probability density functions (PDFs), which are derived from eq. (7), can be rewritten as follows:

$$\begin{aligned} F_1^{\text{exact}} &= \varepsilon \left\{ 1 - \mathrm{P_r}(\gamma_1 > 2^{\frac{R_1}{B}} - 1) \right\} \\ &= \varepsilon \left\{ 1 - \exp\left(-\gamma_1 \left(\frac{1}{\rho \xi_1 \phi_1} \right) \right) \right\} \\ F_2^{\text{exact}} &= \varepsilon \left\{ 1 - \mathrm{P_r}(\gamma_2 > 2^{\frac{R_2}{B}} - 1) \right\} \\ &= \varepsilon \left\{ 1 - \exp\left(-\gamma_2 \left(\frac{1}{\rho \xi_2 (\phi_2 - \phi_1 \gamma_2)} \right) \right) \right\}, \end{aligned} \tag{8}$$

where ξ_i is the mean of fading channel $|h_i|^2$, ε is threshold of connectivity between the UAV and the GU, and $\gamma_i = 2^{R_i} - 1$ is the desired threshold including target rate, R_i. The target rate varies with the transmit SNR ρ and is calculated from eq. (7). For fairness between the CCU and CEU, the bandwidth B is normalized. An explanation of eq. (8) is provided in detail in Appendix A.

Asymptotic approach is derived to describe the limiting behavior of the proposed scheme. For the high SNR ($\rho \to \infty$) approximation where $\exp(x) \approx 1 + x$ for $x \to 0$, the asymptotic expressions can be obtained as follows:

$$\begin{aligned} F_1^{\infty} &= \varepsilon \gamma_1 \left(\frac{1}{\rho \xi_1 \phi_1} \right) \\ F_2^{\infty} &= \varepsilon \gamma_2 \left(\frac{1}{\rho \xi_2 (\phi_2 - \phi_1 \gamma_2)} \right). \end{aligned} \tag{9}$$

2.2.2. Throughput analysis

The maximization of received SNR brings optimization of outage probability performance. In addition, parameters such as SNR, PA coefficients, and target rate affect the outage performance of each user. Thus, the selection of adjusting parameters is important to achieving the desired performance. By using [24] [Eqs. (14)] with some modification, the CDF based throughput can be written as

$$\tau_i = \varepsilon \gamma_i (1 - F_i^{\text{exact}}), \forall_i = 1, 2. \tag{10}$$

From eq. (10), CDFs are substituted into throughput formulations, which can be obtained as follows:

$$\begin{aligned} \tau_1 &= \varepsilon \gamma_1 \exp\left(-\gamma_1 \left(\frac{1}{\rho \xi_1 \phi_1} \right) \right) \\ \tau_2 &= \varepsilon \gamma_2 \exp\left(-\gamma_2 \left(\frac{1}{\rho \xi_2 (\phi_2 - \phi_1 \gamma_2)} \right) \right). \end{aligned} \tag{11}$$

2.2.3. Optimization

The elevation angle and PA coefficients are separately considered to maximize the throughput. The optimization problems should be solved with flexible pairing based on the distances of the UAV and the GU. First, the benefit comes from finding the optimal elevation angle when the UAV is a CEU. Second, finding optimal PA coefficients for a CEU and a CCU is the way to improve performance. In this regard, the optimization problems are formulated as follows:

$$\max_{\theta_2} \ \tau = \tau_1 + \tau_2 \quad \text{subject to } d_{v,U} > d_{v,G} \tag{12a}$$

$$\max_{\phi_1,\phi_2} \ \tau \quad \text{subject to } d_{v,U} < d_{v,G}, \tag{12b}$$

where $d_{v,U}$ and $d_{v,G}$ are vertical distances for the height of UAV and GU. Reverse derivation is needed to solve the problems by minimizing the system outage probability, which carries maximization of the throughput. In addition, the LoS probability help to select the optimal elevation angle, which is changeable based on the environment parameters. The LoS probability calculation is easily derived as a closed form of approximation. The analytical approach is preferred rather than a statistical approach, and it can be approximated to a slightly modified Sigmoid function [25] as follows:

$$P_{LoS}(\theta_i) = \frac{1}{1 + a\exp(-b(\theta_i - a))}, \tag{13}$$

where a and b are environment parameters, which are determined according to the building density and height. In Figure. 2, the LoS probability is shown with four selected environments: Suburban (8,0.45), Urban (15,0.2), Dense Urban (20,0.2), and Highrise Urban (25,0.1) for (a, b).

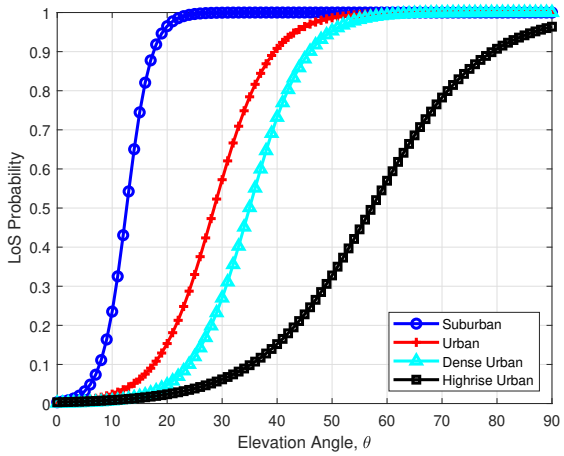

Figure 2. LoS probability with respect to elevation angle.

Differentiation is used to solve the convex problem with respect to ϕ_1 and ϕ_2, the seeking derivation for PA coefficients can be obtained as follows:

$$\begin{aligned} \frac{\partial F_1^{\infty}}{\partial \phi_1} &= -\frac{\Omega}{\rho}\left(\frac{\varepsilon}{\phi_1^2}\right) \\ \frac{\partial F_2^{\infty}}{\partial \phi_2} &= -\frac{\varepsilon\Omega}{\rho(\phi_2 - \phi_1\gamma_2)^2}, \end{aligned} \tag{14}$$

where $\Omega_i = \left(\frac{\gamma_i}{\xi_i}\right)$ and $F^{\infty} = F_1^{\infty} + F_2^{\infty}$. From eq. (13), $\phi_2 - \phi_1\gamma_2 > 0$ term is set to positive and changed to $\gamma_2 < \frac{\phi_2}{\phi_1}$ within $\phi_2 > \phi_1$. The value of γ_2 is the key to selecting PA coefficients where the distance of the UAV is closer than the distance of the GU.

3. Numerical results

In this section, we present the simulated and analytical results to show the performance of the flexible pairing in terms of sum capacity, outage probability, and throughput. The system bandwidth is normalized to $B = 1$ and the radius of a cell is also normalized. Here, the maximum vertical distance is defined as $d_v = 1$ and the connectivity parameter between the UAV and the GU is defined as ε. The total transmit power of the BS is equal to 1 and path loss exponent is 4. The traffic environment is assumed as Urban (15,0.2) where the UAV is assigned as a CEU is located. Based on this condition, the LoS path loss varies with the elevation angle from 10 to 60, and path loss scalar is equal to 23.29. The PA coefficients are fixed as $\phi_1 = 0.2$ and $\phi_1 = 0.8$, where the distances for a CEU and a CCU are $d_1 = 0.2$, $d_2 = 1$. According to the flexible pairing, the role of users can be changed to CCU or CEU. In scenario S1, the CEU is assigned to the UAV and the CCU is assigned to the GU. The scenario S2 is the reverse assignment case.

In Figure 3, the sum capacity comparison with respect to transmit SNR is shown in scenario S1 to compare the effect of LoS effect. The proposed scheme outperforms the conventional where SNR, ρ is below 20[dB].

The sum capacity comparison is shown with respect to difference distance d_1 and d_2 in Figures 4 and 5. In scenario S1, the sum capacity flow is similar between the conventional and proposed scheme. Because the proposed scheme gets less the Los effect when the CCU is the GU.

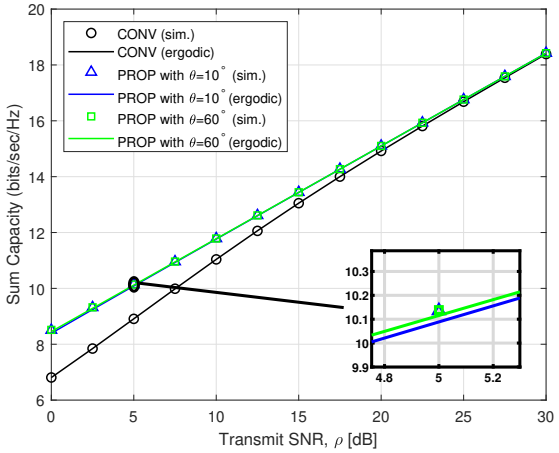

Figure 3. S1: Sum capacity comparison.

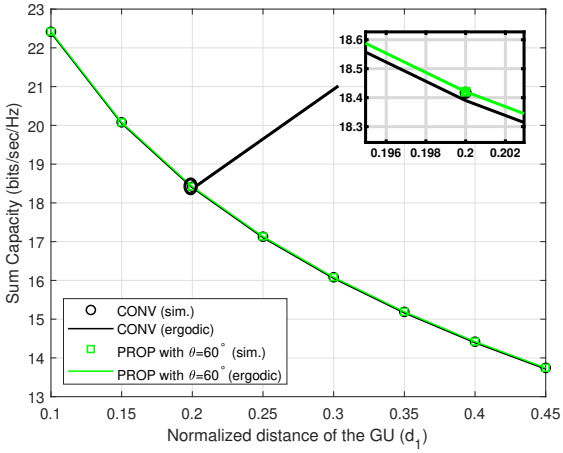

Figure 4. S1: Sum capacity comparison.

In Figure 6, the sum capacity comparison with respect to transmit SNR is shown in scenario S2 to compare relationship between elevation angle and Los effect. The sum capacity is improved by increasing the elevation angle, θ because the LoS effect is more powerful than that of S1. Therefore, it is revealed that the enhancement of sum capacity by adjusting elevation angle is proportional.

The sum capacity comparison is shown with respect to difference distance d_1 and d_2 in Figures 7 and 8. In scenario S2, the sum capacity is dramatically increased compared with that of S1. The sum capacity flow

is similar between the conventional and proposed scheme. Because the proposed scheme gets less the Los effect when the CCU is the GU. The proposed scheme shows saturated capacity which is under the same conditions owing to LoS characteristic.

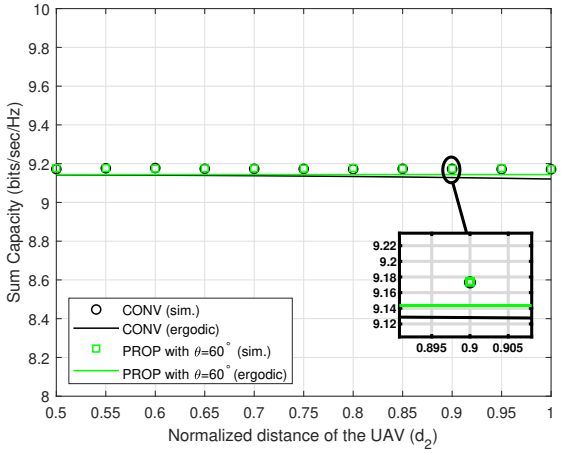

Figure 5. S1: Sum capacity comparison.

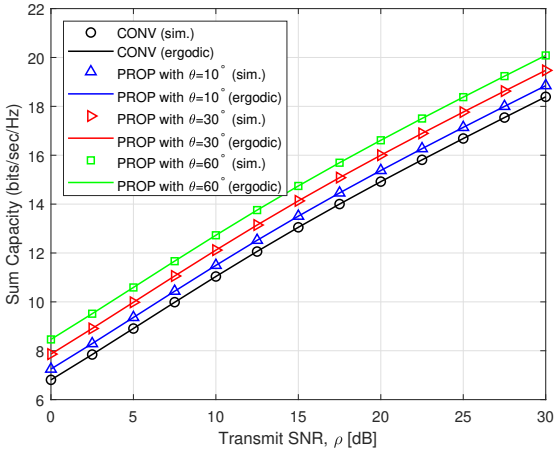

Figure 6. S2: Sum capacity comparison.

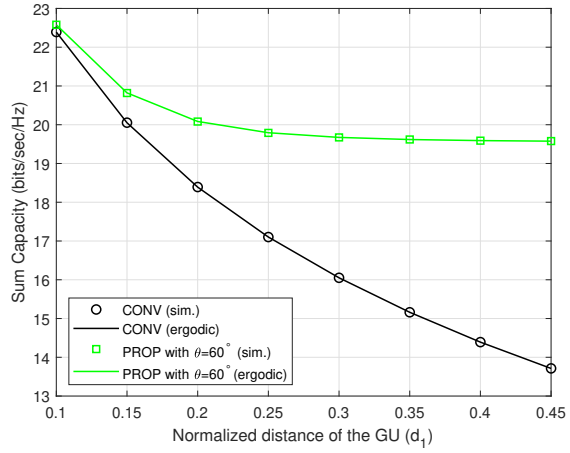

Figure 7. S2: Sum capacity comparison.

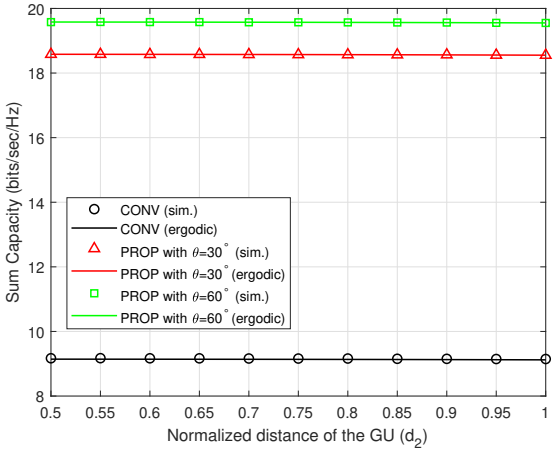

Figure 8. S2: Sum capacity comparison.

In Figure 9, the asymptotic and exact analysis for outage probability are shown to compare the conventional and proposed. The outage probability flow is similar between the conventional and proposed scheme.

In Figure 10, the asymptotic and exact analysis for throughput are shown to compare the conventional and proposed. The proposed scheme outperforms than the conventional when PA coefficients are assigned following to the proposed optimization. Due to difference on achievable capacity, the proposed optimization has higher than that of conventional where the SNR is over 8[dB]. It is evident that there is close saturation after 30[dB], which means the high SNR, because maximum capacity i.e. Shannon's capacity is limited.

In Figure 11, the asymptotic and exact analysis on throughput are shown with respect to connectivity threshold. We assume that the connectivity also is unstable because of switching role of the CCU and the CEU. The throughput performance becomes worse where the connectivity is uncertain, which is same with increasing connectivity threshold.

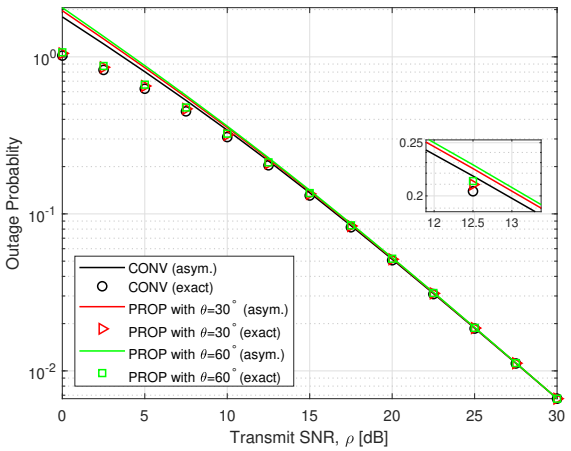

Figure 9. Outage probability comparison.

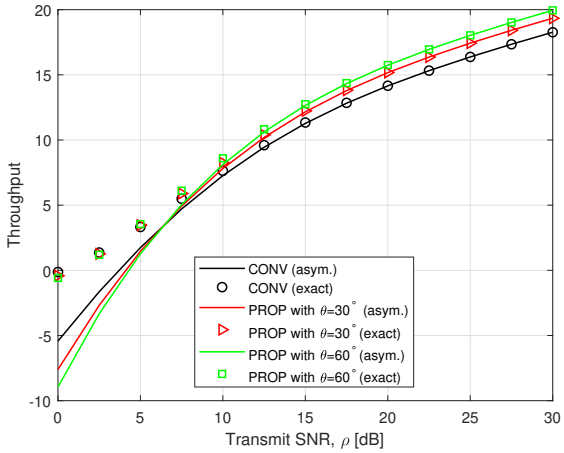

Figure 10. Throughput comparison.

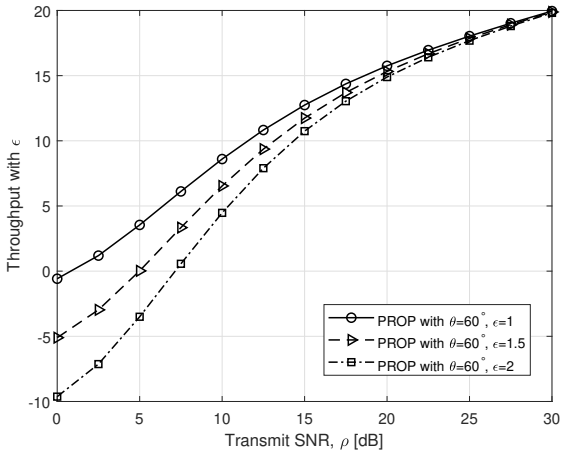

Figure 11. Throughput comparison with ε.

4. Conclusion

In earlier wireless communications, UAV networks have been investigated for the usage of BSs to provide Internet access. However, the proposed approach considers a UAV as one user for pairing in NOMA to maximize the throughput. This paper presents the flexible pairing and channel modeling to solve optimization problems. In addition, we derive analytical and simulated analysis using various performance metrics such as sum capacity, outage probability, and throughput. The performance enhancement is come up with the LoS effect, which determines the channel covariance. Hence, the throughput analysis indicates that the flexible pairing where PA coefficients are assigned following to the proposed optimization outperforms than the conventional scheme. Flexible pairing can be extended to apply other robotic applications by using their mobility to enhance the performance of NOMA. In the future work, multiple UAVs and pairing will be considered to formulate problems.

Acknowledgment

This work was supported by the National Research Foundation of Korea (NRF) grant funded by the Korea government. (MSIT) (No. 2022R1A2B5B01001994).

References

[1] Klaus D,Hendrik B. 6G Vision and Requirements: Is There Any Need for Beyond 5G?. IEEE vehicular technology magazine 2018; 13 (3): 72-80. doi: 10.1109/MVT.2018.2848498

[2] Popovski P, Trillingsgaard KF, Simeone O,Durisi G. 5G wireless network slicing for eMBB, URLLC, and mMTC: A communication-theoretic view. IEEE Access 2018; 6: 55765-55779. doi: 10.1109/ACCESS.2018.2872781

[3] Yuan Y, Yuan Z, Tian L. 5G Non-Orthogonal Multiple Access Study in 3GPP. IEEE Communications Magazine 2020; 58 (7): 90-96. doi: 10.1109/MCOM.001.1900450

[4] Shahab MB,Abbas R,Shirvanimoghaddam M, Sarah J. Grant-Free Non-Orthogonal Multiple Access for IoT: A Survey. IEEE Communications Surveys & Tutorials 2020; 22(3): 1805-1838. doi: 10.1109/COMST.2020.2996032

[5] Makki B,Member S,Chitti K,Behrevan A,Alouini M. A Survey of NOMA: Current Status and Open Research Challenges. IEEE Open Journal of the Communications Society 2020; 1: 179-189. doi: 10.1109/OJCOMS.2020.2969899

[6] Shahab MB,Shin SY. User pairing and power allocation for non-orthogonal multiple access: Capacity maximization under data reliability constraints. Physical Communication 2018; 30: 132-144. doi: 10.1016/j.phycom.2018.05.010

[7] Zhu L, Zhang J, Xiao Z, Cao X, Wu DO. Optimal User Pairing for Downlink Non-Orthogonal Multiple Access (NOMA). IEEE Wireless Communications Letters 2018; 8 (2): 328-331. doi: 10.1109/LWC.2018.2853741

[8] Zhang Q, Jiang M, Feng Z, Li W,Zhang W et al. IoT Enabled UAV: Network Architecture and Routing Algorithm. IEEE Internet of Things Journal 2019; 6 (2): 3727-3742. doi: 10.1109/JIOT.2018.2890428

[9] Qi F, Zhu X, Mang G, Kadoch M, Li W. UAV Network and IoT in the Sky for Future Smart Cities. IEEE Network 2019; 33 (2): 96-101. doi: 10.1109/MNET.2019.1800250

[10] Galkin B, Kibilda J, Luiz A. DaSilva. UAVs as Mobile Infrastructure: Addressing Battery Lifetime. IEEE Communications Magazine 2019; 57 (6): 132-137. doi: 10.1109/MCOM.2019.1800545

[11] Zhang S, Zhang H,He Q,Bian K,Song L. Joint Trajectory and Power Optimization for UAV Relay Networks. IEEE Communications Letters 2017; 22 (1): 161-164. doi: 10.1109/LCOMM.2017.2763135

[12] Cui J, Liu Y, Nallanathan A. Multi-Agent Reinforcement Learning-Based Resource Allocation for UAV Networks. IEEE Transactions on Wireless Communications 2019; 19 (2): 729-743. doi: 10.1109/TWC.2019.2935201

[13] Li X, Wang Q,Peng H, Zhang H, Do DT et al. A Unified Framework for HS-UAV NOMA Networks: Performance Analysis and Location Optimization. IEEE Access 2020; 8: 13329-13340. doi: 10.1109/ACCESS.2020.2964730

[14] Zhao N, Pang X, Li Z, Chen Y, Li F et al. Joint Trajectory and Precoding Optimization for UAV-Assisted NOMA Networks. IEEE Transactions on Communications 2019; 67 (5): 3723-3735. doi: 10.1109/TCOMM.2019.2895831

[15] Liu M, Yang J, Gui G. DSF-NOMA: UAV-Assisted Emergency Communication Technology in a Heterogeneous Internet of Things. IEEE Internet of Things Journal 2019; 6 (3): 5508-5519. doi: 10.1109/JIOT.2019.2903165

[16] Liu X, Wang J,Zhao N, Chen Y,Zhang S et al. Placement and Power Allocation for NOMA-UAV Networks. IEEE Wireless Communications Letters 2019; 8 (3): 965-968. doi: 10.1109/LWC.2019.2904034

[17] Nasir AA,Trung Q. Duong, H. Vincent Poor. UAV-Enabled Communication Using NOMA. IEEE Transactions on Communications 2019; 67 (7): 5126-5138. doi: 10.1109/TCOMM.2019.2906622

[18] Hou T, Liu Y, Song Z, Sun X, Chen Y. Multiple Antenna Aided NOMA in UAV Networks: A Stochastic Geometry Approach. IEEE Transactions on Communications 2018; 67 (2): 1031-1044. doi: 10.1109/TCOMM.2018.2875081

[19] Feng W, Wang J, Chen Y, Wang X, Ning GE et al. UAV-Aided MIMO Communications for 5G Internet of Things. IEEE Internet of Things Journal 2018; 6 (2): 1731-1740. doi: 10.1109/JIOT.2018.2874531

[20] Guo H, Liu J. UAV-Enhanced Intelligent Offloading for Internet of Things at the Edge. IEEE Transactions on Industrial Informatics 2019; 16 (4): 2737-2746. doi: 10.1109/TII.2019.2954944

[21] Series P. Propagation data and prediction methods required for the design of terrestrial broadband radio access systems operating in a frequency range from 3 to 60 GHz, GE, Switzerland: Recommendation ITU-R, 2013.

[22] Mao G, Brian D,Anderson O,Fidan B. WSN06-4: Online Calibration of Path Loss Exponent in Wireless Sensor Networks. In: IEEE Globecom; San Francisco, CA, USA;2006. pp. 1-6.

[23] Shahab MB,Irfan M,Kader MD, Shin SY. User pairing schemes for capacity maximization in non-orthogonal multiple access systems. Wireless Communications and Mobile Computing 2016; 16 (17): 2884-2894. doi: 10.1002/wcm.2736

[24] Singh SK, Agrawa K, Singh K, Li CP. Outage Probability and Throughput Analysis of UAV-Assisted Rate-Splitting Multiple Access. IEEE Wireless Communications Letters 2021; 10 (11): 2528-2532. doi: 10.1109/LWC.2021.3106456

[25] Al-Hourani A, Kandeepan S, Lardner S. Optimal LAP Altitude for Maximum Coverage. IEEE Wireless Communications Letters 2014; 3 (6): 569-572. doi: 10.1109/LWC.2014.2342736

A. Appendix

Derivations of the PDFs $F_1(\gamma_{th})$ and $F_2(\gamma_{th})$.

$$
\begin{aligned}
F_1(\gamma_{th}) &= \mathrm{P_r}\left(\gamma_i\phi_1 \le \gamma_{th}\right) \\
&= \mathrm{P_r}\left(\gamma_i \le \frac{\gamma_{th}}{\phi_1}\right) \\
&= 1 - \mathrm{P_r}\left(\gamma_i \ge \frac{\gamma_{th}}{\phi_1}\right) \\
&= 1 - \mathrm{P_r}\left(1 - F_{\gamma_i}\left(\frac{\gamma_{th}}{\phi_1}\right)\right) \\
&= 1 - \exp^{-\gamma_{th}\left(\frac{1}{\rho\xi_h\phi_1}\right)}
\end{aligned} \tag{15}
$$

$$
\begin{aligned}
F_2(\gamma_{th}) &= \mathrm{P_r}\left(\frac{\gamma_i\phi_2}{\gamma_i\phi_1 + 1} \le \gamma_{th}\right) \\
&= \mathrm{P_r}\left(\gamma_i \le \left(\frac{\gamma_{th}}{\phi_2 - \phi_1\gamma_{th}}\right)\right) \\
&= 1 - \mathrm{P_r}\left(\gamma_i \ge \left(\frac{\gamma_{th}}{\phi_2 - \phi_1\gamma_{th}}\right)\right) \\
&= 1 - \mathrm{P_r}\left(1 - F_{\gamma_i}\left(\frac{\gamma_{th}}{\phi_2 - \phi_1\gamma_{th}}\right)\right) \\
&= 1 - \exp^{-\gamma_{th}\left(\frac{1}{\rho\xi_h(\phi_2 - \phi_1\gamma_{th})}\right)},
\end{aligned} \tag{16}
$$

where the arguments of the functions are nonnegative. The power of exponentials in both functions should guarantee to satisfy the basic PDF and CDF characteristics.